Photon Sidebands of the Ground State and First Excited State of a Quantum Dot

T. H. Oosterkamp, L. P. Kouwenhoven, A. E. A. Koolen, N. C. van der Vaart, and C. J. P. M. Harmans
Department of Applied Physics and Delft Institute of Microelectronics and Submicron-technology (DIMES), Delft University of Technology, P.O. Box 5046, 2600 GA Delft, The Netherlands
(Received 19 July 1996)

We have measured photon-assisted tunneling through a quantum dot with zero dimensional (0D) states. For photon energies smaller than the separation between 0D states we observe photon sideband resonances of the ground state. When the photon energy exceeds the separation between 0D states we observe photon-induced excited state resonances. We identify the different resonances by studying their dependence on photon frequency and magnetic field. [S0031-9007(97)02424-1]

PACS numbers: 73.20.Dx, 73.40.Gk, 73.50.Mx, 73.50.Pz

In analogy to spectroscopy on atoms it is interesting to study the interaction between light and electrons confined in quantum dots. However, since it is difficult to realize identical quantum dots the response of an ensemble of quantum dots to light excitation is strongly averaged over sample differences. Despite this averaging, excitation studies on quantum dot arrays by far-infrared light have shown the spectrum of collective modes [1], and inelastic light scattering experiments have probed single particle excitations [2]. The latter technique has also probed excitons in a single quantum dot [3]. We have used microwaves with relatively low frequency to study the discrete electron excitation spectrum in the conduction band of a single quantum dot. In contrast to the light transmission or luminescence measurements of the above spectroscopy techniques, we measure the photoresponse in the dc current.

Current can flow through a quantum dot when a discrete energy state is aligned to the Fermi energies of the leads. This current is carried by resonant elastic tunneling of electrons between the leads and the dot. An additional time-varying potential $\tilde{V}\cos(2\pi ft)$ can induce *inelastic* tunnel events when electrons exchange photons of energy hf with the oscillating field. This inelastic tunneling with discrete energy exchange is known as photon-assisted tunneling (PAT). PAT has been studied before in superconductor-insulator-superconductor tunnel junctions [4], in superlattices [5], and in quantum dots [6,7]. The quantum dots in Ref. [6] were rather large and effectively had a continuous density of states. So far, PAT through small quantum dots with discrete states has only been studied theoretically [8,9]. In this paper we show for the first time different types of PAT processes through a quantum dot with well resolved discrete 0D states. We first show that an elastic resonant tunneling peak in the current develops photon sideband resonances when we apply microwaves. We then use PAT as a spectroscopic tool to measure the energy evolution of the first excited state as a function of magnetic field [10].

Transport through a quantum dot is dominated by Coulomb blockade effects [11]. The energy to add an extra electron to a quantum dot constitutes the charging energy E_c for a single electron, and a finite energy difference $\Delta\varepsilon$ arising from the confinement. A dot is said to have 0D states if $\Delta\varepsilon$ is larger than the thermal energy k_BT [11]. Assuming sequential tunneling of single electrons, the current can be calculated with a master equation [12]. In Ref. [13] we combine this approach with the Tien-Gordon theory [4] to calculate the effect of microwaves on the dc current through a dot with 0D states. The basic idea is that an ac voltage drop $V = \tilde{V}\cos(2\pi ft)$ over a tunnel barrier modifies the tunnel rate [6]: $\tilde{\Gamma}(E) = \sum_n J_n^2(\alpha)\Gamma(E + nhf)$. Here $\tilde{\Gamma}(E)$ and $\Gamma(E)$ are the tunnel rates at energy E with and without an ac voltage, respectively. $J_n^2(\alpha)$ is the square of the nth order Bessel function evaluated at $\alpha = e\tilde{V}/hf$, which gives the probability that tunneling electrons absorb ($n > 0$) or emit ($n < 0$) n photons of energy hf. In this model the ac electric field is assumed to be confined to the barriers; there are no oscillating electric fields inside the dot or in the leads which could cause transitions within the dot or within the leads. Below we compare some calculations to our measurements.

The diagrams in Fig. 1 show two relevant energy states for N electrons in the dot. For small dc bias voltage and no ac voltages a current resonance occurs when the topmost energy state (i.e., the electrochemical potential) of the quantum dot lines up with the Fermi levels of the leads (see the diagram ε_0). When high frequency voltages drop across the two barriers, additional current peaks appear. We distinguish two mechanisms which were calculated in Ref. [9]. The first mechanism gives photon-induced current peaks when the *separation* between the ground state ε_0 and the Fermi levels of the leads *matches* the photon energy (or nhf), as depicted in the diagrams labeled by $\varepsilon_0 + hf$ and $\varepsilon_0 - hf$. The minus and plus signs correspond to being before or beyond the main resonance. Note that also the case of $\varepsilon_0 - hf$ involves photon absorption. Following the literature on the tunneling time we call these current peaks *sidebands* [14]. The second mechanism leads to photon peaks when an excited state is in resonance with the Fermi levels of the leads (see diagram ε_1). Without PAT, transport

 0031-9007/97/78(8)/1536(4)$10.00

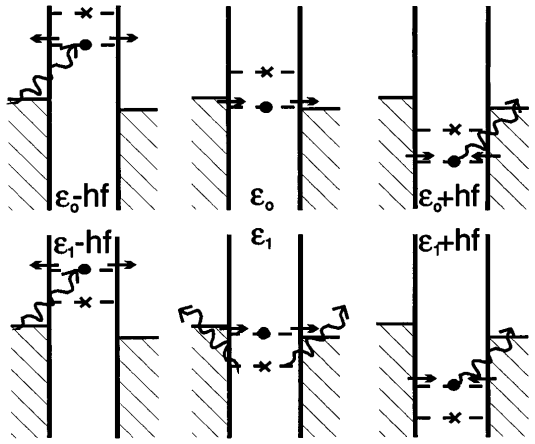

FIG. 1. Diagrams depicting the sequence of tunneling events which dominantly contribute to the current through a quantum dot, for different gate voltages. A small dc bias raises the left Fermi level with respect to the right Fermi level. ε_0 and ε_1 denote the ground state and the first excited state of the N electron system. When the Nth electron tunnels to one of the two reservoirs, the energy states of the dot drop by the charging energy E_c. The corresponding diagrams for $N - 1$ electrons are not shown. Note that only processes with tunneling from or to states close to the Fermi levels in the leads contribute to the net current.

through the excited state ε_1 is blocked since Coulomb blockade prevents having electrons in both the ground state and the excited state simultaneously. The electron in the ground state cannot escape from the dot because its energy is lower than the Fermi levels in the leads. PAT, however, empties the ground state ε_0 when the electron in ε_0 absorbs enough energy and leaves the dot. This process is analogous to photoionization. Now, the Nth electron can tunnel resonantly via the excited state ε_1 as long as the state ε_0 stays empty. Note that for this second mechanism nhf has to *exceed*, but not necessarily *match* the energy splitting $\Delta\varepsilon = \varepsilon_1 - \varepsilon_0$. More photon peaks are generated when these two mechanisms are combined as in the diagrams labeled by $\varepsilon_1 + hf$ and $\varepsilon_1 - hf$. We thus see that PAT can populate the excited states with the help of tunneling between dot and leads. So, even without direct intradot transitions we can perform photon spectroscopy on discrete quantum dot states.

Our measurements are performed on a quantum dot defined by metallic gates (see inset in Fig. 4 below) in a GaAs/AlGaAs heterostructure containing a 2 dimensional electron gas (2DEG) 100 nm below the surface. The 2DEG has mobility 2.3×10^6 cm^2/V s and electron density 1.9×10^{15} m^{-2} at 4.2 K. By applying negative voltages to the two outer pairs of gates, we form two quantum point contacts (QPCs). An additional pair of center gates between the QPCs confines the electron gas to a small dot. No electron transport is possible through the narrow channels between the center gates and the gates forming the QPCs. The center gate voltage V_g can shift the states in the dot with respect to the Fermi levels of the leads and thereby controls the number of electrons in the dot. The energy shift is given by $\Delta E = \kappa \Delta V_g$. A small dc voltage bias is applied between source and drain and the resulting dc source-drain current is measured. From standard dc measurements we find that the effective electron temperature is approximately $T = 200$ mK and the charging energy $E_c = 1.2 \pm 0.1$ meV. We independently determine the level splitting $\Delta\varepsilon$ for different magnetic fields from current-voltage characteristics. In addition to the dc gate voltages we couple a microwave signal (10–75 GHz) capacitatively into one of the center gates.

We concentrate on a single Coulomb peak and study the modification of the shape of the peak induced by the microwave signal [15]. First, we study the photon sidebands of the ground state at a magnetic field $B = 0.84$ T [16]. The main part of Fig. 2 shows measured curves of the current as a function of the gate voltage at different microwave powers for the case $hf < \Delta\varepsilon$ ($hf = 110$ μeV for $f = 27$ GHz and $\Delta\varepsilon = 165$ μeV). Here current flows primarily via the ground state and its photon sidebands (i.e., upper diagrams in Fig. 1). On increasing the microwave power we see in Fig. 2 that the height of the main resonance decreases to zero, while additional resonances develop with increasing amplitude. When we convert gate voltage to energy we find that the additional resonances are located at $\varepsilon_0 \pm hf$ and $\varepsilon_0 \pm 2hf$ [17]. The power dependence is in agreement with the behavior of the Bessel functions: $J_0^2(\alpha)$ for the main resonance ε_0, $J_1^2(\alpha)$ for the one-photon sidebands $\varepsilon_0 \pm hf$, and $J_2^2(\alpha)$ for the two-photon sidebands $\varepsilon_0 \pm 2hf$. For comparison we show a calculation in the inset of Fig. 2 for the same values for the temperature, frequency, and bias voltage as

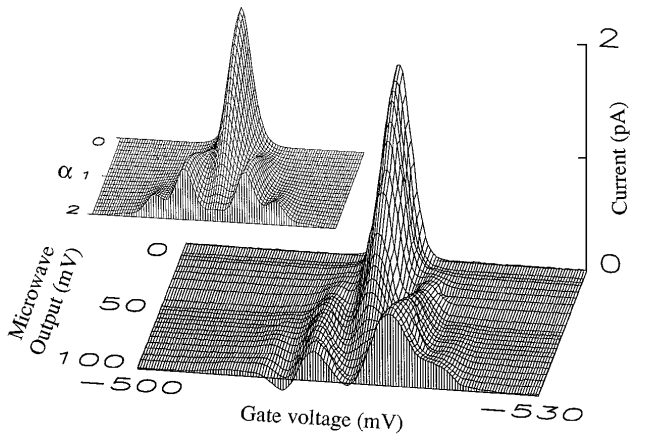

FIG. 2. Measurement of the current through the quantum dot as a function of the center gate voltage and the output voltage of the microwave supply. This data is taken in the single level regime ($hf < \Delta\varepsilon$). $hf = 110$ μeV for $f = 27$ GHz, $\Delta\varepsilon = 165$ μeV at $B = 0.84$ T, and $V = 13$ μV. Note that the gate voltage axis runs from positive to negative. Inset: calculation of the current as a function of the gate voltage and the ac voltage parameter $\alpha = e\tilde{V}/hf$, taking the same values for T, f, and V as in the experiment.

in the experiment. We have assumed equal ac voltages across the two barriers. The small difference between measured and calculated data can be explained if we include an asymmetry in the ac coupling [15].

We now discuss the higher frequency regime where $hf > \Delta\varepsilon$ such that PAT can induce current through excited states. Figure 3 shows measurements of the current at $B = 0.91$ T (here $\Delta\varepsilon = 130$ μeV). In the top section $f = 61.5$ GHz, and in the bottom section $f = 42$ GHz. As we increase the power we see extra peaks coming up. We label the peaks as in Fig. 1. On the right side of the main resonance a new resonance appears, which we assign to photoionization followed by tunneling through the first excited state. At higher powers the one-photon sidebands of the main resonance as well as those of the excited state resonance appear. We do not observe the peak for $\varepsilon_0 + hf$, in this measurement. This can be explained, at least in part, by the fact that here an electron can also tunnel into ε_1 which blocks the photon current through $\varepsilon_0 + hf$. Simulations confirm that the peak for $\varepsilon_0 + hf$ can be several times weaker than the peak for $\varepsilon_0 - hf$ [13]. Also it is masked by the high peak for ε_1 right next to it. The arrows underneath the curves mark the photon energy given by the corresponding frequency. The peaks ε_0 and ε_1 remain in place when we change the frequency, since the photon energy evidently does not alter the energy splitting. The other peaks, $\varepsilon_0 - hf$ and $\varepsilon_1 \pm hf$, shift by an amount which corresponds to the change in photon energy as indicated by the arrows. This reflects that the sidebands originate from matching the states ε_0 and ε_1 to the Fermi levels of the leads by a photon energy hf.

We further substantiate the peak assignment by studying detailed frequency and magnetic field dependence. First, we discuss the frequency scaling. Figure 4 shows the spacing between a resonance and its photon sidebands as a function of the photon energy. Different markers correspond to different photon peaks. The factor $\kappa = 35$ μeV/mV to convert the peak spacings in mV gate voltage into energy is independently determined from dc measurements. The full width at half maximum (FWHM) value of the resonance without microwaves, indicated by the arrow, is proportional to the effective electron temperature in the leads. Structure due to photon energies below this value is washed out by the thermal energy $k_B T$. The frequency scaling firmly establishes PAT as the transport mechanism [4–7]. The observation that the sidebands move linearly with frequency while the ground and excited state resonances stay fixed supports our identification of the different peaks.

We can now use a magnetic field to change the energy separation between the ground state and the first excited state [10] while keeping the distance to the sidebands fixed. Figure 5(a) shows the positions in gate voltage of all observed peaks for 52.5 GHz as a function of magnetic field. The filled circles reflect the evolution of ε_0 with magnetic field. This ground state weakly oscillates with a periodicity of ~80 mT which roughly corresponds to the

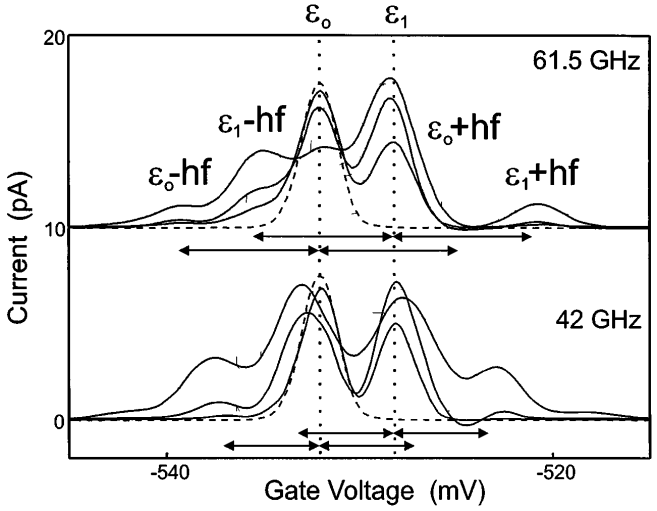

FIG. 3. Measured current as a function of center gate voltage for different microwave powers. The dashed curve is without microwaves. $B = 0.91$ T, $V = 13$ μV, in the top section the frequency is $f = 61.5$ GHz, in the bottom section $f = 42$ GHz. As the frequency of the microwaves is reduced between top and bottom sections, the ground state resonance ε_0 and the resonance attributed to the excited state ε_1 remain at the same gate voltage position. The other peaks, $\varepsilon_0 - hf$ and $\varepsilon_1 \pm hf$, shift inward by an amount which corresponds to the change in photon energy as indicated by the arrows. We do not observe $\varepsilon_0 + hf$ in this measurement.

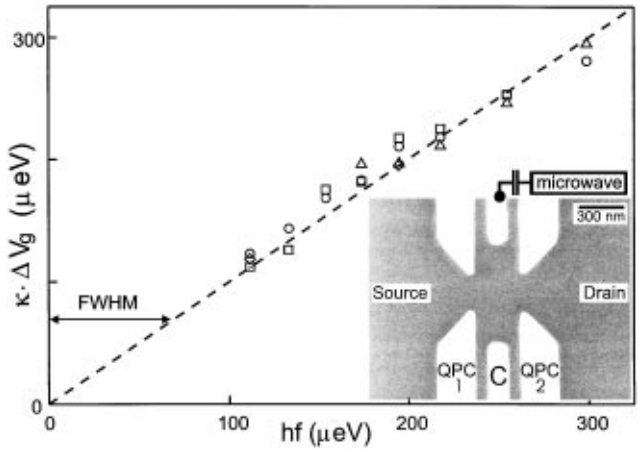

FIG. 4. Peak spacings versus the photon energy. □: spacing between ε_0 and $\varepsilon_0 - hf$. ◇: spacing between ε_0 and $\varepsilon_0 + hf$. △: spacing between ε_1 and $\varepsilon_1 - hf$. ○: spacing between ε_1 and $\varepsilon_1 + hf$. The dashed line is based on the gate voltage to energy conversion factor κ independently determined from dc measurements, and has the theoretically expected slope equal to 1. The arrow indicates the FWHM of the peak. Inset: SEM photo of the sample. The lithographic size of the dot is (600×300) nm^2. Current can flow when we apply a voltage between source and drain. The microwave signal is coupled to one of the center gates.

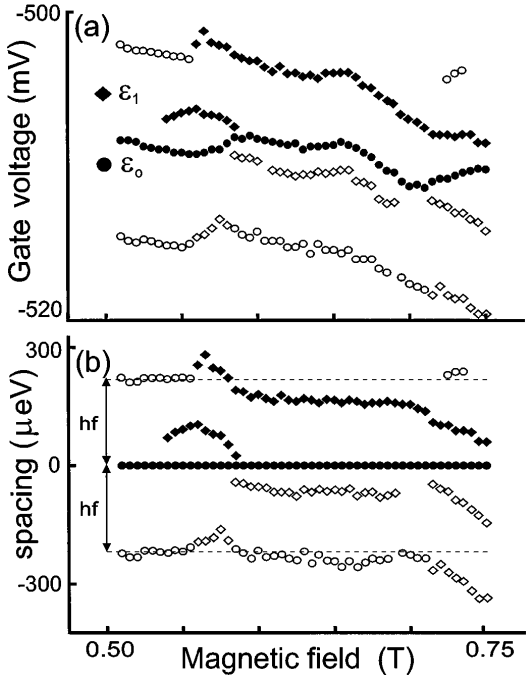

FIG. 5. (a) Peak positions at different magnetic fields at 52.5 GHz. Solid symbols denote peaks which are independent of frequency. Open symbols denote peaks that scale with frequency. (b) Peak spacings relative to the main resonance converted to energy. Closed circles: ε_0; open circles: $\varepsilon_0 \pm hf$; closed diamonds: ε_1; open diamonds: $\varepsilon_1 - hf$ and $\varepsilon_1 - 2hf$.

addition of an extra flux quantum to the dot. The filled diamonds reflect the evolution of ε_1. The open circles (diamonds) show the sidebands $\varepsilon_0 \pm hf$ $(\varepsilon_1 \pm hf)$. Figure 5(b) shows the magnetic field evolution of the excited state and the photon sideband peaks relative to the ground state [i.e., we have subtracted $\varepsilon_0(B)$ from the other curves]. We see that the energy splitting decreases on increasing the magnetic field, and for $0.54 < B < 0.58$ T a degeneracy of the ground state is temporarily lifted and actually two excited states are observed [18]. The dashed lines denote the photon energy $hf = 217$ μeV for 52.5 GHz. The open circles close to these lines are the photon processes $\varepsilon_0 \pm hf$ demonstrating that they indeed move together with the ground state. The open diamonds are the $\varepsilon_1 - hf$ and $\varepsilon_1 - 2hf$ processes. Their motion clearly follows the motion of ε_1. We have thus shown that we can vary the states ε_0 and ε_1 with the magnetic field and, independently, vary the separation to the sidebands with the microwave frequency.

In conclusion, we have used photon-assisted tunneling to study the interaction between microwave light and electrons occupying discrete 0D states in a single quantum dot. The quality of our data shows the feasibility of recently proposed experiments on Rabi-type oscillations between coupled quantum dots [19].

We thank S. F. Godijn, K. Ishibashi, P. Lukey, P. L. McEuen, J. E. Mooij, Yu. V. Nazarov, and T. H. Stoof for discussions and experimental help. We thank Philips Laboratories and C. T. Foxon for providing the heterostructures. The work was supported by the Dutch Foundation for Fundamental Research on Matter (FOM). L.P.K. was supported by the Royal Netherlands Academy of Arts and Sciences (KNAW).

[1] U. Merkt, Physica (Amsterdam) **189B**, 165 (1993), and references therein.
[2] R. Strenz *et al.*, Phys. Rev. Lett. **73**, 3022 (1994), and references therein.
[3] K. Brunner *et al.*, Phys. Rev. Lett. **73**, 1138 (1994).
[4] P. K. Tien and J. R. Gordon, Phys. Rev. **129**, 647 (1963).
[5] P. S. S. Guimares *et al.*, Phys. Rev. Lett. **70**, 3792 (1993); B. J. Keay *et al.*, Phys. Rev. Lett. **75**, 4098 (1995); B. J. Keay *et al.*, Phys. Rev. Lett. **75**, 4102 (1995).
[6] L. P. Kouwenhoven *et al.*, Phys. Rev. B **50**, 2019 (1994); L. P. Kouwenhoven *et al.*, Phys. Rev. Lett. **73**, 3433 (1994).
[7] R. H. Blick *et al.*, Appl. Phys. Lett. **67**, 3924 (1995).
[8] D. Sokolovski, Phys. Rev. B **37**, 4201 (1988).
[9] C. Bruder and H. Schöller, Phys. Rev. Lett. **72**, 1076 (1994).
[10] A. T. Johnson *et al.*, Phys. Rev. Lett. **69**, 1592 (1992).
[11] See for reviews on quantum dots U. Meirav and E. B. Foxman, Semicond. Sci. Technol. **10**, 255 (1995); L. P. Kouwenhoven and P. L. McEuen, in "Nano-Science and Technology," edited by G. Timp (AIP Press, New York, to be published).
[12] D. V. Averin, A. N. Korotkov, and K. K. Likharev, Phys. Rev. B **43**, 6199 (1991); C. W. J. Beenakker, Phys. Rev. B **44**, 1646 (1991).
[13] T. H. Oosterkamp *et al.*, Semicond. Sci. Technol. **11**, 1512 (1996); Phys. Scr. (to be published).
[14] M. Büttiker and R. Landauer, Phys. Rev. Lett. **49**, 1739 (1982).
[15] When the ac voltage drops across the two barriers are unequal, the dot acts as an electron pump [6,9], which makes it more difficult to identify the PAT processes. The amount of pumping turned out to be quite sensitive to the microwave frequency. In order to minimize pumping, frequencies are chosen that do not lead to a dc current in the absence of a dc bias voltage.
[16] PAT is also observed at $B = 0$ but with less resolution due to a higher effective electron temperature at $B = 0$.
[17] Because $2hf > \Delta\varepsilon$ the excited state ε_1 is weakly visible at $V_g \sim -508$ mV in Fig. 2 where it overlaps with $\varepsilon_0 + 2hf$.
[18] Our measurement of the evolution of the excited state ε_1 agrees with the data in Fig. 4 of Ref. [10] and in Fig. 11 of P. L. McEuen *et al.*, Physica (Amsterdam) **189B**, 70 (1993). However, we do not know of a theory that properly describes the observed magnetic field dependence of excited states.
[19] T. H. Stoof and Yu. V. Nazarov, Phys. Rev. B **53**, 1050 (1996); C. A. Stafford and N. S. Wingreen, Phys. Rev. Lett. **76**,1916 (1996).